JHEP

Published for SISSA by Springer

Received: October 26, 2015
Accepted: December 14, 2015
Published: December 28, 2015

Lepton flavor violating radiative decays in EW-scale ν_R model: an update

P.Q. Hung,[a,d] **Trinh Le,**[a] **Van Que Tran**[b] **and Tzu-Chiang Yuan**[c,e]

[a] *Department of Physics, University of Virginia, Charlottesville, VA 22904-4714, U.S.A.*
[b] *Department of Physics, National Taiwan Normal University, Taipei 116, Taiwan*
[c] *Institute of Physics, Academia Sinica, Nangang, Taipei 11529, Taiwan*
[d] *Center for Theoretical and Computational Physics, Hue University College of Education, Hue, Vietnam*
[e] *Physics Division, National Center for Theoretical Sciences, Hsinchu, Taiwan*

E-mail: pqh@virginia.edu, ttl9ve@virginia.edu, apc.tranque@gmail.com, tcyuan@phys.sinica.edu.tw

Abstract: We perform an updated analysis for the one-loop induced charged lepton flavor violating radiative decays $l_i \to l_j \gamma$ in an extended mirror model. Mixing effects of the neutrinos and charged leptons constructed with a horizontal A_4 symmetry are also taken into account. Current experimental limit and projected sensitivity on the branching ratio of $\mu \to e\gamma$ are used to constrain the parameter space of the model. Calculations of two related observables, the electric and magnetic dipole moments of the leptons, are included. Implications concerning the possible detection of mirror leptons at the LHC and the ILC are also discussed.

Keywords: Rare Decays, Beyond Standard Model

ArXiv ePrint: 1508.07016

doi:10.1007/JHEP12(2015)169

JHEP12(2015)169

Contents

JHEP12(2015)169

1 Introduction

The electroweak-scale right-handed neutrino (EW-scale ν_R) model was proposed in ref. [1] with the following main motivations in mind: 1) To provide a model for the see-saw mechanism which can be realized at the electroweak scale instead of a typical grand unification theory (GUT) scale; 2) To be able to test the seesaw mechanism through the discovery of right-handed neutrinos whose Majorana masses are now bounded by the electroweak scale $\Lambda_{\rm EW} \sim 246\,{\rm GeV}$; 3) To be able to probe at high energies (e.g. at the Large Hadron Collider (LHC)) lepton-number violating processes such as like-sign dilepton events coming from the Majorana nature of the right-handed neutrinos. The electroweak-scale right-handed neutrinos belong to doublets of the Standard Model (SM) SU(2) whose partners are right-handed "heavy" mirror charged leptons. The requirement of the absence of anomaly dictates the addition of right-handed doublets of mirror quarks to the particle spectrum. Furthermore, left-handed SU(2)-singlet mirror quarks and mirror charged leptons will be the counterparts of their SM right-handed SU(2)-singlet quarks and charged leptons.

The EW-scale ν_R model entails extra SU(2) chiral doublets (the mirror fermions) which have many consequences. These mirror fermions have an impact on various quantities and processes such as the electroweak precision parameters, rare processes, etc. at the loop level.

The first type of effects that needs to be examined is the contributions of these extra chiral doublets to the electroweak precision parameters. These calculations have been performed in [2] and it was found that there is a large parameter space where the EW-scale ν_R model satisfies the EW precision constraints. In a nutshell, the contributions from the mirror fermions are partially cancelled by those of the scalar sector, in particular the SU(2) triplet scalar.

The next place where mirror fermions enter through loop corrections is rare processes such as $\mu \to e\,\gamma$ and $\tau \to \mu\,\gamma$. In [3], such processes have been discussed in a generic fashion, with an emphasis on the possible correlation between the observability of the aforementioned rare processes and the decay lengths of the mirror charged leptons, both of which are of phenomenological interest. In this article, we will present an update of the process $\mu \to e\,\gamma$ taking into account recent developments of the model, including experimental inputs from the recently-discovered 125 GeV SM-like scalar [4, 5]. They are summarized below.

The scalar sector of the original model [1] contains one SM-like Higgs doublet and two Higgs triplets, one with $Y/2 = 1$ containing doubly-charged scalars and one with $Y/2 = 0$. (The rationale for this sector will be explained in the summary section.) The discovery of the 125 GeV SM-like scalar has opened up a whole new chapter on any model beyond the SM, in particular those models which have more than one Higgs doublet. In light of this discovery, a close examination of the scalar sector of the EW-scale ν_R model [6] revealed that its original Higgs content is insufficient to accommodate the 125 GeV SM-like scalar. In light of this issue, ref. [6] introduced an additional Higgs doublet besides the original doublet: one of which couples to the SM fermions and the other one to the mirror quarks and charged leptons. This yields two 125-GeV candidates with one being SM-like (dubbed *Dr. Jekyll*) and the other being very different (*Mr. Hyde*), both of which giving comparable signal strengths in agreement with ATLAS and CMS data.

Most importantly for the present manuscript is the recent work [7] concerning neutrino and SM charged lepton masses and mixings. The fact that the SM lepton mixing matrix $U_{\rm PMNS}$ (the Pontecorvo-Maki-Nakagawa-Sakata mixing matrix) is so different from the quark counterpart, $V_{\rm CKM}$ (the Cabibbo-Kobayashi-Maskawa mixing matrix), has given rise to many models, many of which invoke the presence of some kind of discrete symmetry. Among these different proposals for the discrete symmetry is the popular A_4 symmetry which has been used to reproduce the tribimaximal form of $U_{\rm PMNS}$. This symmetry is usually applied to the charged lepton sector [8–10] and involves four or more Higgs doublets. (Such a large number of Higgs doublets might be hard to accommodate the 125 GeV SM-like scalar with the desired observed properties.) The new twist of [7] is to exhibit the A_4 symmetry in the neutrino Dirac mass sector and the scalar sector involved is composed of $\mathrm{SU}(2)\times\mathrm{U}(1)_Y$-singlet scalars which are not constrained by LHC data. These singlet scalars are composed of a singlet and a triplet of A_4. This model reproduces the desired PMNS matrix and makes predictions on the charged lepton mass matrix in the form of $\mathcal{M}_l\mathcal{M}_l{}^\dagger$.

JHEP12(2015)169

The singlet scalars play a crucial role in the process $\mu \to e\,\gamma$ in the EW-scale ν_R model as shown in [3] and updated below in light the aforementioned developments. The results presented in this paper contain a deep correlation between the branching ratio $B(\mu \to e\,\gamma)$ and the neutrino sector in the form of the PMNS matrix for both normal and inverted hierarchies, as well as the form of the mirror lepton mixing matrix. It will be shown that the exclusion zones in the plots of the branching ratio of $B(\mu \to e\,\gamma)$ versus the Yukawa coupling strengths to the singlets depend a bit on how strong the A_4-triplet scalars couple to the leptons.

This paper is organized as follows. First, in section 2, we summarize the essence of the EW-scale ν_R model (original [1] and extended [6]). Next, in section 3, we briefly review constraints from electroweak precision measurements for the original model and from Higgs physics for the extended model. In section 4, we briefly review the results of neutrino and charged lepton masses and mixings [7]. We then proceed with the actual calculations of the process $l_i \to l_j\gamma$, the anomalous magnetic dipole moment Δa_{l_i} and the electric dipole moment d_{l_i} for the lepton l_i in section 5. Detailed numerical analysis will be presented in section 6. Implications of our results concerning the possible detection of mirror leptons at the LHC and the ILC are discussed in section 7. We finally summarize and conclude in section 8. A few useful formulas are collected in an appendix.

2 Review of the EW-scale ν_R model

For the sake of clarity, we review in this section the original EW-scale ν_R model [1] and its extended version [6].

- Gauge group:

$$\mathrm{SU}(3)_C \times \mathrm{SU}(2) \times \mathrm{U}(1)_Y \tag{2.1}$$

  There are many differences between the EW-scale ν_R model and the popular Left-Right symmetric model [11–14]. The first difference lies in the gauge structure of the two models: $\mathrm{SU}(3)_C \times \mathrm{SU}(2) \times \mathrm{U}(1)_Y$ for the EW-scale ν_R model and $\mathrm{SU}(3)_C \times \mathrm{SU}(2)_L \times \mathrm{SU}(2)_R \times \mathrm{U}(1)_{B-L}$ for the Left-Right model.

- Lepton and quark SU(2) doublets (the superscript M refer to mirror fermions):

  SM: $l_L = \begin{pmatrix} \nu_L \\ e_L \end{pmatrix}$; Mirror: $l_R^M = \begin{pmatrix} \nu_R^M \\ e_R^M \end{pmatrix}$.

  SM: $q_L = \begin{pmatrix} u_L \\ d_L \end{pmatrix}$; Mirror: $q_R^M = \begin{pmatrix} u_R^M \\ d_R^M \end{pmatrix}$.

- Lepton and quark SU(2) singlets:

  SM: e_R; u_R, d_R; Mirror: e_L^M; u_L^M, d_L^M.

JHEP12(2015)169

- Doublet Higgs fields:

  As explained in [1], a Higgs doublet is needed to give masses to all *charged* fermions. The analysis of the properties of the 125-GeV SM-like scalar necessitates the introduction of one extra Higgs doublet as explained in [6]. Each Higgs doublet couples to a different sector: $\Phi_2 = (\phi_2^+, \phi_2^0)$ to the SM fermions and $\Phi_{2M} = (\phi_{2M}^+, \phi_{2M}^0)$ to the mirror fermions. They develop the following vacuum-expectation-values (VEV): $\langle\Phi_2\rangle = (0, v_2/\sqrt{2})^T$ and $\langle\Phi_{2M}\rangle = (0, v_{2M}/\sqrt{2})^T$.

- Triplet Higgs fields:

  The SU(2)-triplet Higgs fields form the cornerstone of the EW-scale ν_R model. As shown in [1], the VEV of the $Y/2 = 1$ triplet gives an electroweak-scale Majorana mass to the right-handed neutrinos and the $Y/2 = 0$ triplet is needed to preserve the custodial symmetry so that the ρ parameter equals unity at tree level. This is summarized below. Here we just write down the triplet Higgs fields and their VEVs.

  - $\widetilde{\chi}\ (Y/2 = 1) = \frac{1}{\sqrt{2}}\ \vec{\tau}.\vec{\chi} = \begin{pmatrix} \frac{1}{\sqrt{2}}\chi^+ & \chi^{++} \\ \chi^0 & -\frac{1}{\sqrt{2}}\chi^+ \end{pmatrix}$ with $\langle\chi^0\rangle = v_M$.
  - $\xi\ (Y/2 = 0) = (\xi^+, \xi^0, \xi^-)$ (in order to restore Custodial Symmetry) with $\langle\xi^0\rangle = v_M$.
  - VEVs:
    $v_2^2 + v_{2M}^2 + 8v_M^2 = v^2 \approx (246\,\mathrm{GeV})^2$.

- Singlet Higgs fields:

  The original model which is basically concerned with the energy scales which enter the seesaw mechanism contains only one $\mathrm{SU}(2) \times \mathrm{U}(1)_Y$-singlet Higgs field ϕ_S whose VEV $\langle\phi_S\rangle = v_S$ gives the Dirac mass to the neutrinos (to be summarized below). It turns out that this choice was insufficient to discuss lepton mixings and, in particular, the PMNS matrix U_{PMNS}. This problem has been recently investigated by [7] within the framework of an A_4 symmetry which is applied to the neutrino sector of the EW-scale ν_R model. The upshot of this study was the introduction of an A_4 singlet ϕ_{0S} and an A_4-triplet $\{\phi_{iS}\}$ $(i = 1, 2, 3)$. They obtain the following VEVs v_0 and v_i respectively. We will summarize below the main points concerning this singlet scalar sector in the construction of U_{PMNS} and its implication to rare processes such as $\mu \to e\gamma$.

- Dirac neutrino mass

  For simplicity, we will denote the right-handed neutrino fields by ν_R from hereon. The original model contains one singlet scalar whose VEV provides a Dirac mass for the neutrinos. A generic Yukawa coupling is of the form

$$\begin{aligned} \mathcal{L}_S &= -g_{Sl}\,\bar{l}_L\ \phi_S\ l_R^M + \mathrm{H.c.} \\ &= -g_{Sl}(\bar{\nu}_L\ \nu_R\ + \bar{e}_L\ e_R^M)\ \phi_S + \mathrm{H.c.} \end{aligned} \tag{2.2}$$

  With $\langle\phi_S\rangle = v_S$, one obtains the Dirac mass $m_\nu^D = g_{Sl}\ v_S$.

JHEP12(2015)169

- Majorana neutrino mass

  The electroweak-scale Majorana mass for the right-handed neutrinos is obtained from the following coupling

$$\begin{aligned} -\mathcal{L}_M &= g_M \, l_R^{M,T} \, \sigma_2 \, \tau_2 \, \tilde{\chi} \, l_R^M \\ &= g_M \, \nu_R^T \, \sigma_2 \, \nu_R \, \chi^0 - \frac{1}{\sqrt{2}} \, \nu_R^T \, \sigma_2 \, e_R^M \, \chi^+ \\ &\quad - \frac{1}{\sqrt{2}} \, e_R^{M,T} \, \sigma_2 \, \nu_R \, \chi^+ + e_R^{M,T} \, \sigma_2 \, e_R^M \, \chi^{++} \, . \end{aligned} \tag{2.3}$$

  With $\langle \chi^0 \rangle = v_M$, the Majorana mass is given by $M_R = g_M v_M$.

3 Review of results of the EW-scale ν_R model

In this review section, we will discuss two sets of results for the EW-scale ν_R model obtained in [2] (the electroweak precision constraints) and [6] (constraints from the 125-GeV SM-like scalar).

3.1 Electroweak precision constraints on the EW-scale ν_R model

The presence of mirror quark and lepton SU(2)-doublets can, by themselves, seriously affect the constraints coming from electroweak precision data. As noticed in [2], the positive contribution to the S-parameter coming from the extra right-handed mirror quark and lepton doublets could be partially cancelled by the negative contribution coming from the triplet Higgs fields. Ref. [2] has carried out a detailed analysis of the electroweak precision parameters S and T and found that there is a large parameter space in the model which satisfies the present constraints and that there is no fine tuning due to the large size of the allowed parameter space. It is beyond the scope of the paper to show more details here but a representative plot would be helpful. Figure 1 shows the contribution of the scalar sector versus that of the mirror fermions to the S-parameter within 1σ and 2σ. In this plot, [2] took for illustrative purpose 3500 data points that fall inside the 2σ blue region with about 100 data points falling inside the 1σ red region. More details can be found in [2].

3.2 Review of the scalar sector of the EW-scale ν_R model in light of the discovery of the 125-GeV SM-like scalar

In light of the discovery of the 125-GeV SM-like scalar, it is imperative that any model beyond the SM (BSM) shows a scalar spectrum that contains at least one Higgs field with the desired properties as required by experiment. The present data from CMS and ATLAS only show signal strengths that are compatible with the SM Higgs boson. The definition of a signal strength μ is as follows

$$\mu(H\text{-decay}) = \frac{\sigma(H\text{-decay})}{\sigma_{\rm SM}(H\text{-decay})} \, , \tag{3.1}$$

with

$$\sigma(H\text{-decay}) = \sigma(H\text{-production}) \times B(H\text{-decay}) \, . \tag{3.2}$$

JHEP12(2015)169

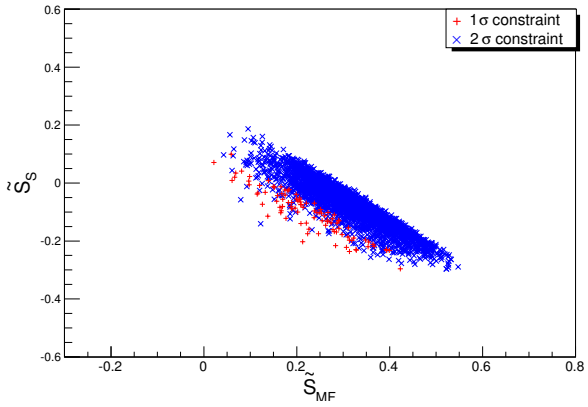

Figure 1. Constrained $\tilde{S}_S$ versus $\tilde{S}_{\rm MF}$.

To really distinguish the SM Higgs field from its impostor, it is necessary to measure the partial decay widths and the various branching ratios. In the present absence of such quantities, the best one can do is to present cases which are consistent with the experimental signal strengths. This is what was carried out in [6].

The minimization of the potential containing the scalars shown above breaks its global symmetry $\mathrm{SU}(2)_L \times \mathrm{SU}(2)_R$ down to a custodial symmetry $\mathrm{SU}(2)_D$ which guarantees at tree level $\rho = M_W^2/M_Z^2 \cos^2\theta_W = 1$ [6]. The physical scalars can be grouped, based on their transformation properties under $\mathrm{SU}(2)_D$ as follows:

$$\begin{aligned} \text{five-plet (quintuplet)} &\to H_5^{\pm\pm},\ H_5^{\pm},\ H_5^0; \\ \text{triplet} &\to H_3^{\pm},\ H_3^0; \\ \text{triplet} &\to H_{3M}^{\pm},\ H_{3M}^0; \\ \text{three singlets} &\to H_1^0,\ H_{1M}^0,\ H_1^{0\prime}\,. \end{aligned} \tag{3.3}$$

The three custodial singlets are the CP-even states, one combination of which can be the 125-GeV scalar. In terms of the original fields, one has $H_1^0 = \phi_2^{0r}$, $H_{1M}^0 = \phi_{2M}^{0r}$ and $H_1^{0\prime} = \frac{1}{\sqrt{3}}\left(\sqrt{2}\chi^{0r} + \xi^0\right)$. These states mix through a mass matrix obtained from the potential and the mass eigenstates are denoted by $\widetilde{H}$, $\widetilde{H}'$ and $\widetilde{H}''$, with the convention that the lightest of the three is denoted by $\widetilde{H}$, the next heavier one by $\widetilde{H}'$ and the heaviest state by $\widetilde{H}''$.

To compute the signal strengths μ, ref. [6] considers $\widetilde{H} \to ZZ$, W^+W^-, $\gamma\gamma$, $b\bar{b}$ and $\tau\bar{\tau}$. In addition, the cross section of $gg \to \widetilde{H}$ related to $\widetilde{H} \to gg$ was also calculated. A scan over the parameter space of the model yielded *two interesting scenarios* for the 125-GeV scalar: 1) *Dr. Jekyll*'s scenario in which $\widetilde{H} \sim H_1^0$ meaning that the SM-like component $H_1^0 = \phi_2^{0r}$ is *dominant*; 2) *Mr. Hyde*'s scenario in which $\widetilde{H} \sim H_1^{0\prime}$ meaning that the SM-like component $H_1^0 = \phi_2^{0r}$ is *subdominant*. Both scenarios give signal strengths compatible with experimental data as shown below in figure 2.

JHEP12(2015)169

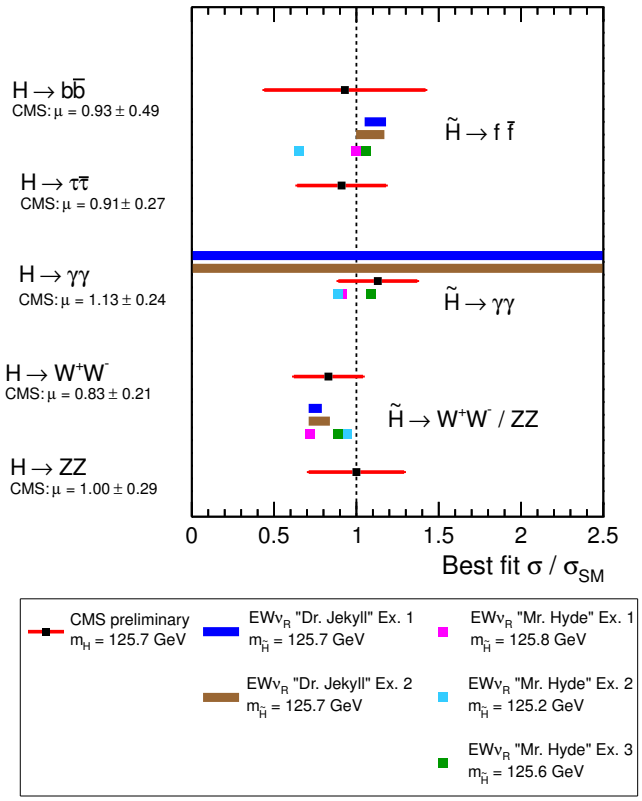

Figure 2. Predictions of signal strength $\mu(\widetilde{H} \to b\bar{b},\ \tau\bar{\tau},\ \gamma\gamma,\ W^+W^-,\ ZZ)$ in the EW-scale ν_R model for examples 1 and 2 in *Dr. Jekyll* and example 1, 2 and 3 in *Mr. Hyde* scenarios as discussed in [6], in comparison with corresponding best fit values by CMS [15–18].

As we can see from figure 2, both SM-like scenario (*Dr. Jekyll*) and the *more interesting scenario* which is very unlike the SM (*Mr. Hyde*) agree with experiment. As stressed in [6], present data cannot tell whether or not the 125-GeV scalar is truly SM-like or even if it has a dominant SM-like component. It has also been stressed in [6] that it is essential to measure the partial decay widths of the 125-GeV scalar to truly reveal its nature. Last but not least, in both scenarios, $H^0_{1M} = \phi^{0r}_{2M}$ is subdominant but is essential to obtain the agreement with the data as shown in [6].

As discussed in detail in [6], for proper vacuum alignment, the potential contains a term proportional to λ_5 (eq. (32) of [6]) and it is this term that prevents the appearance of Nambu-Goldstone (NG) bosons in the model. The would-be NG bosons acquire a mass proportional to λ_5.

An analysis of CP-odd scalar states H^0_3, H^0_{3M} and the heavy CP-even states $\widetilde{H}', \widetilde{H}''$ was presented in [6]. The phenomenology of charged scalars including the doubly-charged ones was also discussed in [19].

The phenomenology of mirror quarks and leptons was briefly discussed in [2] and a detailed analysis of mirror quarks is presented in [20]. It suffices to mention here that mirror fermions decay into SM fermions through the process $q^M \to q\phi_S$, $l^M \to l\phi_S$ with ϕ_S

JHEP12(2015)169

"appearing" as missing energy in the detector. Furthermore, the decay of mirror fermions into SM ones can happen outside the beam pipe and inside the silicon vertex detector. Searches for non-SM fermions do not apply in this case. It is beyond the scope of the paper to discuss these details here.

4 Review of neutrino and charged lepton masses and mixings in the EW-scale ν_R model

Since the ideas and notations coming out of this review will be important for the calculation of the rate of $\mu \to e\gamma$, we will present a little more details than the previous section.

In [7], a model of the Dirac part of neutrino masses was constructed using the widely popular A_4 symmetry. Unlike previous works on that symmetry where there was a need to introduce several (more than two and typically four or five) Higgs doublets (see the review by [8–10]) and where it might be very problematic with the discovery of the 125-GeV SM-like scalar, the main motivation of [7] is to first obtain the Cabibbo-Wolfenstein matrix [21, 22]

$$U_{CW} = \frac{1}{\sqrt{3}} \begin{pmatrix} 1 & 1 & 1 \\ 1 & \omega & \omega^2 \\ 1 & \omega^2 & \omega \end{pmatrix}, \tag{4.1}$$

which is a prototype of the PMNS matrix with "large" mixing parameters and which, upon a slight modification, could reproduce the "experimental" $U_{\rm PMNS}$ being defined as

$$U_{\rm PMNS} = U_\nu^\dagger U_L^l \,. \tag{4.2}$$

Under A_4, $(\nu, l)_L$, $(\nu, l^M)_R$, e_R and e_L^M transform as $\underline{3}$, where e and ν are generic notations for the charged and neutral leptons. Using the A_4 multiplication rule $\underline{3} \times \underline{3} = \underline{1}(11 + 22 + 33) + \underline{1}'(11 + \omega^2 22 + \omega 33) + \underline{1}''(11 + \omega 22 + \omega^2 33) + \underline{3}(23, 31, 12) + \underline{3}(32, 13, 21)$ with $\omega = e^{i2\pi/3}$, it was argued in [7] that the appropriate set of singlet scalars is composed of an A_4 singlet ϕ_{0S} and an A_4-triplet $\{\phi_{iS}\}$ $(i = 1, 2, 3)$. To reflect the two different ways that the A_4-triplet can couple to the leptons, [7] wrote down the Lagrangian

$$\mathcal{L}_S = -\bar{l}_L^0 \left(g_{0S}\phi_{0S} + g_{1S}\tilde{\phi}_S + g_{2S}\tilde{\phi}_S\right) l_R^{M,0} + \text{H.c.}\,, \tag{4.3}$$

where l_L^0 and $l_R^{M,0}$ are gauge eigenstates which are related to the mass eigenstates by

$$l_L^0 = U_L^l l_L \,, \qquad l_R^{M,0} = U_R^{l^M} l_R^M \,. \tag{4.4}$$

Using the aforementioned multiplication rule, one obtains the following matrix

$$M_\phi = \begin{pmatrix} g_{0S}\phi_{0S} & g_{1S}\phi_{3S} & g_{2S}\phi_{2S} \\ g_{2S}\phi_{3S} & g_{0S}\phi_{0S} & g_{1S}\phi_{1S} \\ g_{1S}\phi_{2S} & g_{2S}\phi_{1S} & g_{0S}\phi_{0S} \end{pmatrix} . \tag{4.5}$$

As shown in [7], reality of neutrino Dirac masses implies that

$$g_{2S} = g_{1S}^* \,. \tag{4.6}$$

JHEP12(2015)169

Furthermore, it was shown that, with $v_0 = \langle \phi_{0S} \rangle$ and $v_i = \langle \phi_{iS} \rangle = v$, the neutrino mass matrix

$$M_\nu^D = \begin{pmatrix} g_{0S}v_0 & g_{1S}v_3 & g_{2S}v_2 \\ g_{2S}v_3 & g_{0S}v_0 & g_{1S}v_1 \\ g_{1S}v_2 & g_{2S}v_1 & g_{0S}v_0 \end{pmatrix} , \tag{4.7}$$

can be diagonalized, i.e. $U_\nu^\dagger M_\nu^D U_\nu$, by the matrix

$$U_\nu = \frac{1}{\sqrt{3}} \begin{pmatrix} 1 & 1 & 1 \\ 1 & \omega^2 & \omega \\ 1 & \omega & \omega^2 \end{pmatrix} . \tag{4.8}$$

Notice that $U_\nu \equiv U_{CW}^\dagger$. Eqs. (4.8) and (4.5) will form a basis for our subsequent discussion.

For the purpose of the subsequent sections, we rewrite eq. (4.3) as follows

$$\mathcal{L}_S = -\bar{l}_L \, U_L^{l\dagger} U_\nu U_\nu^\dagger M_\phi U_\nu U_\nu^\dagger U_R^{l^M} \, l_R^M + \text{H.c.} \tag{4.9}$$

$$= -\bar{l}_L \, U_{\text{PMNS}}^\dagger \, \tilde{M}_\phi \, U_{\text{PMNS}}^M l_R^M + \text{H.c.} \, , \tag{4.10}$$

where

$$\tilde{M}_\phi = U_\nu^\dagger M_\phi U_\nu \, , \tag{4.11}$$

and

$$U_{\text{PMNS}}^M = U_\nu^\dagger U_R^{l^M} \, . \tag{4.12}$$

The above construction can be straightforwardly generalized for the right-handed leptons and left-handed mirror leptons. Hence the total $\mathcal{L}_S$ becomes

$$\mathcal{L}_S = -\bar{l}_L \, U_{\text{PMNS}}^\dagger \, \tilde{M}_\phi \, U_{\text{PMNS}}^M l_R^M - \bar{l}_R \, U_{\text{PMNS}}^{\prime\dagger} \, \tilde{M}'_\phi \, U_{\text{PMNS}}^{\prime M} l_L^M + \text{H.c.} \tag{4.13}$$

where $\tilde{M}'_\phi = U_\nu^\dagger M'_\phi U_\nu$ and M'_ϕ is the same as M_ϕ given by eq. (4.5) with $g_{0S} \to g'_{0S}$, $g_{1S} \to g'_{1S}$ and $g_{2S} \to g'_{2S}$. Reality of the eigenvalues of M'_ϕ also implies $g'_{2S} = g'^*_{1S}$. In analogous to U_{PMNS} and U_{PMNS}^M, we have defined the following mixing matrices for the second term of eq. (4.13)

$$U'_{\text{PMNS}} = U_\nu^\dagger U_R^l \, , \tag{4.14}$$

and

$$U_{\text{PMNS}}^{\prime M} = U_\nu^\dagger U_L^{l^M} \, , \tag{4.15}$$

where U_R^l and $U_L^{l^M}$ are the unitary matrices relating the gauge eigenstates and the mass eigenstates

$$l_R^0 = U_R^l l_R \, , \quad l_L^{M,0} = U_L^{l^M} l_L^M \, . \tag{4.16}$$

5 The calculation

The one-loop irreducible diagram for $l_i \to l_j \gamma$ is shown in figure 3. Other two diagrams related to wave function renormalization are not explicitly shown. However they are crucial for the cancellation of ultraviolet divergences and obtaining gauge invariance results in our

JHEP12(2015)169

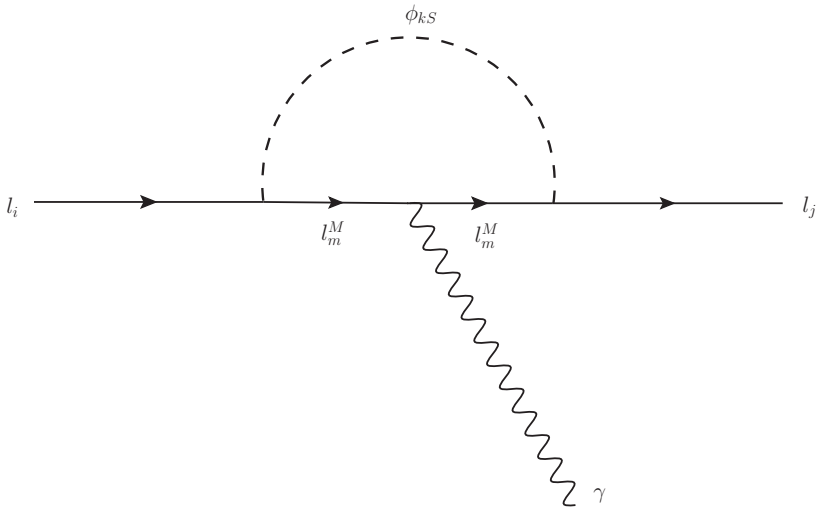

Figure 3. One-loop induced Feynman diagram for $l_i \to l_j\gamma$ in EW-scale ν_R model.

calculation. The relevant Yukawa couplings between the leptons, mirror leptons and the A_4 singlet and triplet scalars can be deduced by recasting the Lagrangian $\mathcal{L}_S$ in eq. (4.13) into the following component form

$$\mathcal{L}_S = -\sum_{k=0}^{3}\sum_{i,m=1}^{3}\left(\bar{l}_{Li}\,\mathcal{U}_{im}^{L\,k}\,l_{Rm}^{M} + \bar{l}_{Ri}\,\mathcal{U}_{im}^{R\,k}\,l_{Lm}^{M}\right)\phi_{kS} + \text{H.c.} \tag{5.1}$$

where

$$\mathcal{U}_{im}^{L\,k} \equiv \left(U_{\text{PMNS}}^{\dagger}\cdot M^{k}\cdot U_{\text{PMNS}}^{l^M}\right)_{im}\,, \tag{5.2}$$

$$= \sum_{j,n=1}^{3}\left(U_{\text{PMNS}}^{\dagger}\right)_{ij} M_{jn}^{k}\left(U_{\text{PMNS}}^{M}\right)_{nm}\,, \tag{5.3}$$

and

$$\mathcal{U}_{im}^{R\,k} \equiv \left(U_{\text{PMNS}}^{\prime\,\dagger}\cdot M^{\prime\,k}\cdot U_{\text{PMNS}}^{\prime\,l^M}\right)_{im}\,, \tag{5.4}$$

$$= \sum_{j,n=1}^{3}\left(U_{\text{PMNS}}^{\prime\,\dagger}\right)_{ij} M_{jn}^{\prime\,k}\left(U_{\text{PMNS}}^{\prime\,M}\right)_{nm}\,. \tag{5.5}$$

The matrix elements for the four matrices $M^k(k = 0, 1, 2, 3)$ are listed in table 1. $M_{jn}^{\prime\,k}$ can be obtained from M_{jn}^{k} listed in table 1 with the following substitutions $g_{0S} \to g_{0S}^{\prime}$ and $g_{1S} \to g_{1S}^{\prime}$.

We note that due to the suppression by small neutrino mass insertion the contributions from SM gauge boson loops [23–27] are in general quite small and they will be ignored from our analysis.

JHEP12(2015)169

M^k_{jn}	Value
$M^0_{12}, M^0_{13}, M^0_{21}, M^0_{23}, M^0_{31}, M^0_{32}$	0
$M^0_{11}, M^0_{22}, M^0_{33}$	g_{0S}
$M^1_{11}, M^2_{11}, M^3_{11}$	$\frac{2}{3}\mathrm{Re}\left(g_{1S}\right)$
$M^1_{22}, M^2_{22}, M^3_{22}$	$\frac{2}{3}\mathrm{Re}\left(\omega^* g_{1S}\right)$
$M^1_{33}, M^2_{33}, M^3_{33}$	$\frac{2}{3}\mathrm{Re}\left(\omega g_{1S}\right)$
M^1_{12}, M^1_{21}	$\frac{2}{3}\mathrm{Re}\left(\omega g_{1S}\right)$
M^2_{12}, M^3_{21}	$\frac{1}{3}\left(g_{1S} + \omega g^*_{1S}\right)$
M^3_{12}, M^2_{21}	$\frac{1}{3}\left(g^*_{1S} + \omega^* g_{1S}\right)$
M^1_{13}, M^1_{31}	$\frac{2}{3}\mathrm{Re}\left(\omega^* g_{1S}\right)$
M^2_{13}, M^3_{31}	$\frac{1}{3}\left(g_{1S} + \omega^* g^*_{1S}\right)$
M^3_{13}, M^2_{31}	$\frac{1}{3}\left(g^*_{1S} + \omega g_{1S}\right)$
M^1_{23}, M^1_{32}	$\frac{2}{3}\mathrm{Re}\left(g_{1S}\right)$
M^2_{23}, M^3_{32}	$\frac{2\omega^*}{3}\mathrm{Re}\left(g_{1S}\right)$
M^3_{23}, M^2_{32}	$\frac{2\omega}{3}\mathrm{Re}\left(g_{1S}\right)$

Table 1. Matrix elements for $M^k (k = 0, 1, 2, 3)$.

5.1 The process $l_i \to l_j \gamma$ $(i \neq j)$ in EW-scale ν_R model

Lorentz and gauge invariance dictate the form of the amplitude for the process $l_i^-(p) \to l_j^-(p') + \gamma(q)$ to be

$$\mathcal{M}\left(l_i^- \to l_j^- \gamma\right) = \epsilon^*_\mu(q)\bar{u}_j(p')\left\{i\sigma^{\mu\nu}q_\nu\left[C_L^{ij}P_L + C_R^{ij}P_R\right]\right\}u_i(p)\,, \tag{5.6}$$

where $P_{L,R} = (1 \mp \gamma_5)/2$. The coefficients $C^{ij}_{L,R}$ can be extracted from the one-loop diagram (figure 3),

$$\begin{aligned} C_L^{ij} = &+\frac{e}{16\pi^2}\sum_{k=0}^{3}\sum_{m=1}^{3}\left\{\frac{1}{m^2_{l_m^M}}\left[m_i \mathcal{U}^{Rk}_{jm}\left(\mathcal{U}^{Rk}_{im}\right)^* + m_j \mathcal{U}^{Lk}_{jm}\left(\mathcal{U}^{Lk}_{im}\right)^*\right]\mathcal{I}\left(\frac{m^2_{\phi_{kS}}}{m^2_{l_m^M}}\right)\right. \\ &\left. + \frac{1}{m_{l_m^M}}\mathcal{U}^{Rk}_{jm}\left(\mathcal{U}^{Lk}_{im}\right)^*\mathcal{J}\left(\frac{m^2_{\phi_{kS}}}{m^2_{l_m^M}}\right)\right\}, \end{aligned} \tag{5.7}$$

$$\begin{aligned} C_R^{ij} = &+\frac{e}{16\pi^2}\sum_{k=0}^{3}\sum_{m=1}^{3}\left\{\frac{1}{m^2_{l_m^M}}\left[m_i \mathcal{U}^{Lk}_{jm}\left(\mathcal{U}^{Lk}_{im}\right)^* + m_j \mathcal{U}^{Rk}_{jm}\left(\mathcal{U}^{Rk}_{im}\right)^*\right]\mathcal{I}\left(\frac{m^2_{\phi_{kS}}}{m^2_{l_m^M}}\right)\right. \\ &\left. + \frac{1}{m_{l_m^M}}\mathcal{U}^{Lk}_{jm}\left(\mathcal{U}^{Rk}_{im}\right)^*\mathcal{J}\left(\frac{m^2_{\phi_{kS}}}{m^2_{l_m^M}}\right)\right\}. \end{aligned} \tag{5.8}$$

Here we have assumed the mirror lepton masses are much larger than the external fermion masses $m_{l_m^M} \gg m_{i,j}$ and set $m_{i,j} \to 0$ in the loop functions $\mathcal{I}(r)$ and $\mathcal{J}(r)$, which are simply

JHEP12(2015)169

given by

$$\mathcal{I}(r) = \frac{1}{12(1-r)^4}\left[-6r^2\log r + r(2r^2+3r-6)+1\right], \tag{5.9}$$

$$\mathcal{J}(r) = \frac{1}{2(1-r)^3}\left[-2r^2\log r + r(3r-4)+1\right]. \tag{5.10}$$

In our numerical work for $\mu \to e\gamma$ presented in section 6, we will consider the mirror lepton masses of the order a few hundred GeV and the A_4 singlet and triplet scalar masses of the order 10 MeV, thus the ratio $r = m^2_{\phi_{kS}}/m^2_{l^M_m} \sim 10^{-8}$ is very tiny. For all practical purposes, one can replace eqs. (5.9) and (5.10) by the limits $\lim_{r\to 0}\mathcal{I}(r) = 1/12$ and $\lim_{r\to 0}\mathcal{J}(r) = 1/2$ respectively. Formulas of $\mathcal{I}$ and $\mathcal{J}$ for the general case of $m_{i,j} \neq 0$ are given in the appendix.

The partial width for $l_i \to l_j\gamma$ is given by

$$\Gamma\left(l_i \to l_j\gamma\right) = \frac{1}{16\pi}m^3_{l_i}\left(1-\frac{m^2_{l_j}}{m^2_{l_i}}\right)^3\left(|C^{ij}_L|^2 + |C^{ij}_R|^2\right). \tag{5.11}$$

5.2 Magnetic dipole moment

The magnetic dipole moment anomaly for lepton l_i can be easily extracted from the above calculation with the following result

$$\begin{aligned}\Delta a_{l_i} &= \frac{2m_{l_i}}{e}\left(\frac{C^{ii}_L + C^{ii}_R}{2}\right)\\ &= +\frac{1}{16\pi^2}\left\{\sum_{k=0}^{3}\sum_{m=1}^{3} 2\left(|\mathcal{U}^{Lk}_{im}|^2 + |\mathcal{U}^{Rk}_{im}|^2\right)\frac{m^2_{l_i}}{m^2_{l^M_m}}\mathcal{I}\left(\frac{m^2_{\phi_{kS}}}{m^2_{l^M_m}}\right)\right.\\ &\quad \left. + \sum_{k=0}^{3}\sum_{m=1}^{3}\mathrm{Re}\left(\mathcal{U}^{Lk}_{im}\left(\mathcal{U}^{Rk}_{im}\right)^*\right)\frac{m_{l_i}}{m_{l^M_m}}\mathcal{J}\left(\frac{m^2_{\phi_{kS}}}{m^2_{l^M_m}}\right)\right\}.\end{aligned} \tag{5.12}$$

5.3 Electric dipole moment

The electric dipole moment operator for a fermion f is usually defined as

$$\mathcal{L}_{\mathrm{EDM}} = -i\frac{d_f}{2}\bar{f}\sigma^{\mu\nu}\gamma_5 f F_{\mu\nu}\,, \tag{5.13}$$

where $F_{\mu\nu}$ is the electromagnetic field strength and the coefficient d_f the electric dipole moment. The electric dipole moment for lepton l_i can also be easily extracted from the above calculation with the result

$$\begin{aligned}d_{l_i} &= \frac{i}{2}\left(C^{ii}_L - C^{ii}_R\right),\\ &= +\frac{e}{16\pi^2}\sum_{k=0}^{3}\sum_{m=1}^{3}\frac{1}{m_{l^M_m}}\mathrm{Im}\left(\mathcal{U}^{Lk}_{im}\left(\mathcal{U}^{Rk}_{im}\right)^*\right)\mathcal{J}\left(\frac{m^2_{\phi_{kS}}}{m^2_{l^M_m}}\right).\end{aligned} \tag{5.14}$$

JHEP12(2015)169

6 Numerical analysis

The branching ratio $\mathrm{B}(\mu \to e\gamma)$ is given by

$$\mathrm{B}(\mu \to e\gamma) = \tau_\mu \cdot \Gamma\left(\mu \to e\gamma\right) \tag{6.1}$$

where τ_μ is the lifetime of the muon [28]

$$\tau_\mu = (2.1969811 \pm 0.0000022) \times 10^{-6}\ \mathrm{s}\ . \tag{6.2}$$

In our numerical analysis, we will adopt the following approach:

- For the masses of the singlet scalars ϕ_{kS}, we take

  $$m_{\phi_{0S}} : m_{\phi_{1S}} : m_{\phi_{2S}} : m_{\phi_{3S}} = M_S : 2M_S : 3M_S : 4M_S$$

  with a fixed common mass $M_S = 10\,\mathrm{MeV}$. As long as $m_{\phi_{kS}} \ll m_{l_m^M}$, our results will not be affected much by the exact mass relations among these singlet scalars.

- For the masses of the mirror lepton l_m^M, we take

  $$m_{l_m^M} = M_{\mathrm{mirror}} + \delta_m$$

  with $\delta_1 = 0$, $\delta_2 = 10\,\mathrm{GeV}$, $\delta_3 = 20\,\mathrm{GeV}$ and vary the common mass M_{mirror} from $100\,\mathrm{GeV}$ to $800\,\mathrm{GeV}$.

- We assume all the Yukawa couplings g_{0S}, g_{1S}, g_{2S}, g'_{0S}, g'_{1S}, and g'_{2S} to be all real.[1] As mentioned before, $g_{2S} = (g_{1S})^*$ and $g'_{2S} = (g'_{1S})^*$ due to the reality of the mass eigenvalues of the Dirac neutrino masses. For simplicity, we also take $g_{0S} = g'_{0S}$, $g_{1S} = g'_{1S}$ and study the following 6 cases:

  1. $g_{0S} \neq 0,\ g_{1S} = 0$. The A_4 triplet terms are switched off.
  2. $g_{1S} = 10^{-2} \times g_{0S}$. The A_4 triplet couplings are merely one percent of the singlet ones.
  3. $g_{1S} = 10^{-1} \times g_{0S}$. The A_4 triplet couplings are 10 percent of the singlet ones.
  4. $g_{1S} = 0.5 \times g_{0S}$. The A_4 triplet couplings are one half of the singlet ones.
  5. $g_{1S} = g_{0S}$. Both A_4 singlet and triplet terms have the same weight.
  6. $g_{0S} = 0,\ g_{1S} \neq 0$. The A_4 singlet terms are switched off.

- For the three unknown mixing matrices U^M_{PMNS}, U'_{PMNS} and U'^M_{PMNS}, we will consider two scenarios:

  – Scenario 1

  $$U^M_{\mathrm{PMNS}} = U'_{\mathrm{PMNS}} = U'^M_{\mathrm{PMNS}} = U^\dagger_{CW}$$

[1] In this study, we do not analyze the possibility of electric dipole moments for the charged leptons in which complex Yukawa couplings must be assumed.

JHEP12(2015)169

– Scenario 2

$$U^{M}_{\rm PMNS} = U'_{\rm PMNS} = U'^{M}_{\rm PMNS} = U_{\rm PMNS}$$

Recall that the standard parameterization of the PMNS matrix is given by

$$U_{\rm PMNS} = \begin{pmatrix} c_{12}c_{13} & s_{12}c_{13} & s_{13}e^{-i\delta} \\ -s_{12}c_{23} - c_{12}s_{23}s_{13}e^{i\delta} & c_{12}c_{23} - s_{12}s_{23}s_{13}e^{i\delta} & s_{23}c_{13} \\ s_{12}s_{23} - c_{12}c_{23}s_{13}e^{i\delta} & -c_{12}s_{23} - s_{12}c_{23}s_{13}e^{i\delta} & c_{23}c_{13} \end{pmatrix} \cdot P$$

where $s_{ij} \equiv \sin\theta_{ij}$, $c_{ij} \equiv \cos\theta_{ij}$ and $P = \mathrm{Diag}(1, e^{i\alpha_{21}/2}, e^{i\alpha_{31}/2})$ is the Majorana phase matrix. We will ignore the Majorana phases in this analysis.

In table 2 we list the 1σ range of the mixing parameters as given by the recent analysis of global three-neutrino oscillation data in [29, 30]. With the central values for the mixing parameters given in table 2 as inputs, we obtain two possible solutions of the PMNS matrix:

$$U^{\rm NH}_{\rm PMNS} = \begin{pmatrix} 0.8221 & 0.5484 & -0.0518 + 0.1439i \\ -0.3879 + 0.07915i & 0.6432 + 0.0528i & 0.6533 \\ 0.3992 + 0.08984i & -0.5283 + 0.05993i & 0.7415 \end{pmatrix}$$

for normal hierarchy, and

$$U^{\rm IH}_{\rm PMNS} = \begin{pmatrix} 0.8218 & 0.5483 & -0.08708 + 0.1281i \\ -0.3608 + 0.0719i & 0.6467 + 0.04796i & 0.6664 \\ 0.4278 + 0.07869i & -0.5254 + 0.0525i & 0.7293 \end{pmatrix}$$

for inverted hierarchy. For each scenario, we consider these two possible solutions for the $U_{\rm PMNS}$. Due to the small differences between these two solutions, we expect our results are not too sensitive to the neutrino mass hierarchies.

- Limits on $B(\mu \to e\gamma)$ from MEG experiment [31] and its projected sensitivity [32]:

$$B(\mu \to e\gamma) \leq 5.7 \times 10^{-13}\ (90\,\%\text{C.L.})[\text{MEG, 2013}]\ , \tag{6.3}$$

$$B(\mu \to e\gamma) \sim 4 \times 10^{-14}\ [\text{Projected Sensitivity}]\ . \tag{6.4}$$

- Δa_μ from E821 experiment [33]:

$$\Delta a_\mu \equiv a_\mu^{\rm exp} - a_\mu^{\rm SM} = 288(63)(49) \times 10^{-11}\ . \tag{6.5}$$

Since the dominant contributions to the loop amplitude arise from the mass insertion of the internal mirror lepton line in figure 3, only the last terms in eqs. (5.7), (5.8) and (5.12) are significant numerically. As long as $m_{\phi_{kS}} \ll m_{l^M_m}$, the current MEG limit (eq. (6.3)) on the branching ratio $B(\mu \to e\gamma)$ imposes the constraint

$$\left|\sum_{k,m} \mathcal{U}^{R\,k}_{1m} \left(\mathcal{U}^{L\,k}_{2m}\right)^* \left(\frac{100\,\text{GeV}}{m_{l^M_m}}\right)\right|^2 + \left|\sum_{k,m} \mathcal{U}^{L\,k}_{1m} \left(\mathcal{U}^{R\,k}_{2m}\right)^* \left(\frac{100\,\text{GeV}}{m_{l^M_m}}\right)\right|^2 \leq 7.9 \times 10^{-19}\ ,$$

JHEP12(2015)169

Mixing Parameters	Normal Hierarchy	Inverted Hierarchy
$\sin^2\theta_{12}$	0.308 ± 0.017	0.308 ± 0.017
$\sin^2\theta_{23}$	$0.437^{+0.033}_{-0.023}$	$0.455^{+0.139}_{-0.031}$
$\sin^2\theta_{13}$	$0.0234^{+0.0020}_{-0.0019}$	$0.024^{+0.0019}_{-0.0022}$
δ/π	$1.39^{+0.38}_{-0.27}$	$1.31^{+0.29}_{-0.33}$
$\delta m^2 = m_2^2 - m_1^2$	$(7.54^{+0.26}_{-0.22}) \times 10^{-5}\text{eV}^2$	$(7.54^{+0.26}_{-0.22}) \times 10^{-5}\text{eV}^2$
$\Delta m^2 = \lvert m_3^2 - (m_1^2 + m_2^2)/2\rvert$	$(2.43 \pm 0.06) \times 10^{-3}\text{eV}^2$	$(2.38 \pm 0.06) \times 10^{-3}\text{eV}^2$

Table 2. Mixing parameters from global three-neutrino oscillation data taken from [29, 30].

while the result from the Brookhaven E821 experiment on Δa_μ (eq. (6.5)) imposes

$$\sum_{k,m} \text{Re}\left(\mathcal{U}_{2m}^{L\,k}\left(\mathcal{U}_{2m}^{R\,k}\right)^*\right)\left(\frac{100\,\text{GeV}}{m_{l_m^M}}\right) \leq 8.6\times 10^{-4}\,.$$

In figures 4–9 we plot the contour of $\text{Log}_{10}B(\mu \to e\gamma)$ (upper panel) and $\text{Log}_{10}\Delta a_\mu$ (bottom panel) in the $(g_{0S\,\text{or}\,1S}, M_{\text{mirror}})$ plane for both normal (left panel) and inverted (right panel) neutrino mass hierarchies for scenarios 1 (red curves) and 2 (blue curves) with the six cases of couplings aforementioned: (1) $g_{0S} \neq 0,\ g_{1S} = 0$ (figure 4), (2) $g_{1S} = 10^{-2} \times g_{0S}$ (figure 5), (3) $g_{1S} = 10^{-1} \times g_{0S}$ (figure 6), (4) $g_{1S} = 0.5 \times g_{0S}$ (figure 7), (5) $g_{0S} = g_{1S}$ (figure 8), and (6) $g_{0S} = 0,\ g_{1S} \neq 0$ (figure 9), respectively.

At the upper panel of each of these figures, the (light) gray area is excluded by the current limit of $\text{Log}_{10}B(\mu \to e\gamma) = -12.24$ from MEG experiment [31] for scenario (1) 2 respectively. The projected sensitivity of $\text{Log}_{10}B(\mu \to e\gamma) = -13.40$ [32] is also shown for each scenario in the two plots in the upper panel for comparison.

At the bottom panel of each of these figures, the red (blue) area is defined by the $\text{Log}_{10}\Delta a_\mu = -8.54$ [33] from the E821 experiment of the Brookhaven National Lab (BNL) for the discrepancy between the SM model prediction and the measurement for the muon anomalous magnetic dipole moment for scenario 1 (2), respectively.

From all the plots in these figures, we observe the following general features.

- In the same mass range of the mirror leptons the LFV process $\mu \to e\gamma$ is more sensitive to the couplings by almost two order of magnitudes as compared with the anomalous magnetic dipole moment of the muon. This is partly due to the fact that the $B(\mu \to e\gamma)$ is quartic in the couplings, while in Δa_μ they are quadratic.

- As one turns on the A_4 triplet coupling g_{1S} from 0 to $g_{1S} = g_{0S}$ (figure 4 to figure 8), the contours for $\text{Log}_{10}B(\mu \to e\gamma)$ (upper panels) are shifting toward to the left, indicating the role of the triplet singlets become more relevant and thus the constraints on parameter space become more stringent from the current MEG limit. However in the last case of figure 9 when the A_4 singlet coupling g_{0S} is set to zero such that only the triplet singlets are contributing in the loop diagram, the contours of $\text{Log}_{10}B(\mu \to e\gamma)$ are slightly shifting back toward to the right. Similar behaviors

JHEP12(2015)169

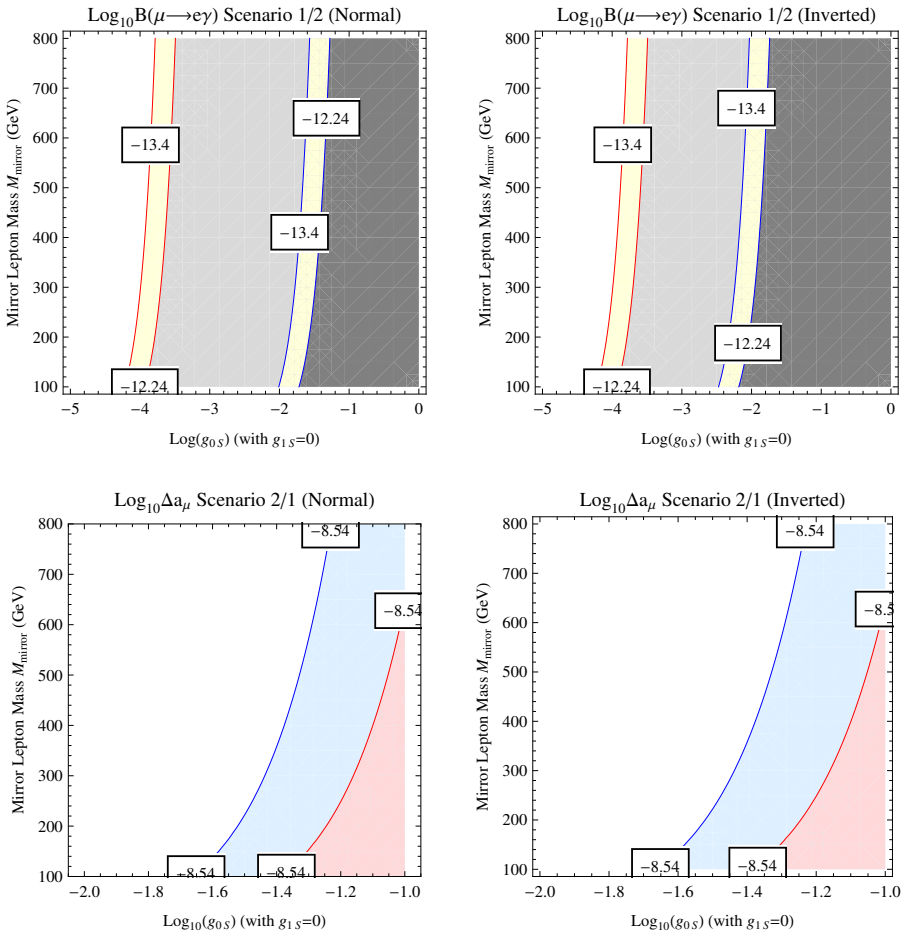

Figure 4. Contour plots of $\mathrm{Log}_{10}B(\mu \to e\gamma)$ (top panel) and $\mathrm{Log}_{10}\Delta a_\mu$ (bottom panel) on the $(g_{0S}, M_{\rm mirror})$ plane for normal (left panel) and inverted (right panel) hierarchy in scenarios 1 (red curves) and 2 (blue curves) with $g_{0S} = g'_{0S}$ and $g_{1S} = g'_{1S} = 0$. For details of other input parameters, one can refer to the text in section 6.

can be found for the contours of $\mathrm{Log}_{10}\Delta a_\mu$, but the effects are tiny and not easily seen on the log scale, except for the last three cases of figures 7–9 (lower panels).

Regarding the sensitivity on the two scenarios, we can obtain the following statement by comparing the red and blue contours corresponding to the scenarios 1 and and 2 in each of these figures.

- The sensitivity of the couplings in the $B(\mu \to e\gamma)$ has been weakened by one to two order of magnitudes for scenario 2 as compared to scenario 1. This is due to the fact that in scenario 2, the three unknown unitary mixing matrices are now departure from $U^\dagger_{CW}$, which allows the couplings take on larger values since the amplitudes involve products of the couplings and the elements of mixing matrices. However this sensitivity is not present for the muon anomalous magnetic dipole moment as the distance between the two red and blue contours for the two scenarios in the lower

JHEP12(2015)169

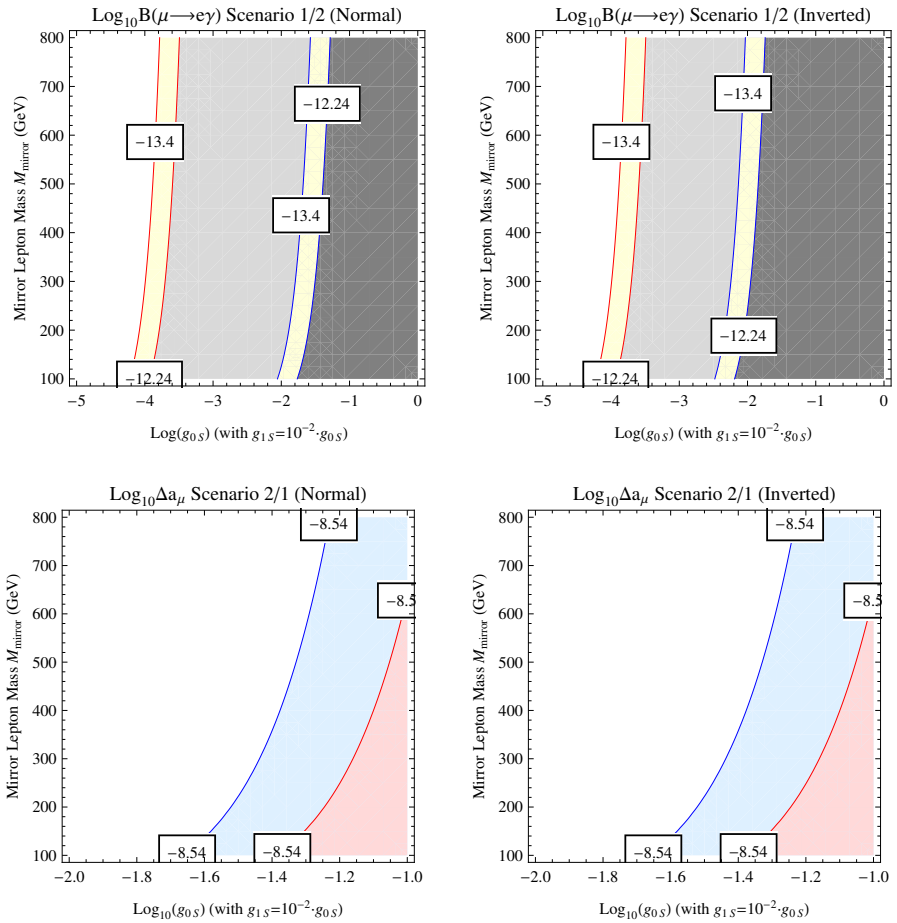

Figure 5. Same as figure 4 with $g_{0S} = g'_{0S}$ and $g_{1S} = g'_{1S} = 10^{-2} \cdot g_{0S}$ instead.

panels of all these plots are well within a small range of the coupling g_{0S} (or g_{1S} in figure 9). For example, at $M_{\rm mirror} = 100\,{\rm GeV}$, the allowed value of g_{0S} varies from $10^{-4.5}$ to $10^{-1.8}$ ($10^{-1.9}$ to $10^{-1.4}$) as seen from the upper (lower) panels of figures 4–8.

Regarding the sensitivity on the neutrino mass hierarchies, one can obtain the following statements by comparing the left and right panels in each of these figures.

- As one slowly turns on the A_4 triplet coupling $g_{1S} = 0$ (figure 4) to $g_{1S} = 10^{-1} \times g_{0S}$ (figure 6), the red contours of ${\rm Log}_{10}B(\mu \to e\gamma)$ of scenario 1 in the left and right panels in all these plots remain the same, while the blue contours of scenario 2 in the right panels move toward to the left. This indicates that noticeable differences in the contours of ${\rm Log}_{10}B(\mu \to e\gamma)$ between the normal and inverted neutrino mass hierarchies can be seen in these cases. In general the couplings are about an order of magnitude more sensitive in the inverted mass hierarchy than the normal one for scenario 2. However, for $g_{1S} \geq 0.5 \times g_{0S}$, these differences diminish.

- There are no discernible differences between the two mass hierarchies for the muon anomalous magnetic dipole moment in both scenarios for all 6 cases of couplings.

JHEP12(2015)169

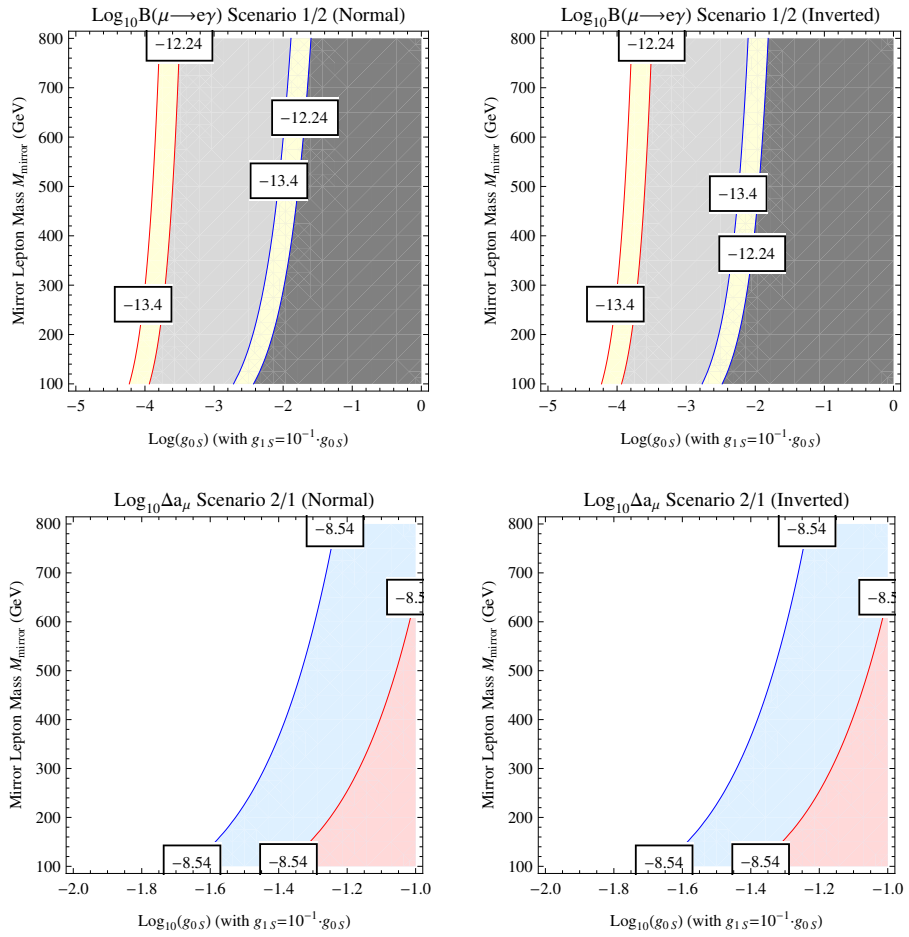

Figure 6. Same as figure 4 with $g_{0S} = g'_{0S}$ and $g_{1S} = g'_{1S} = 10^{-1} \cdot g_{0S}$ instead.

7 Implications

The constraints on the Yukawa couplings coming from $\mu \to e\gamma$ has several implications among which two are particularly relevant.

- The size allowed for the Yukawa couplings by present limits on $B(\mu \to e\gamma)$ has an important implication on the decay lengths of the mirror leptons. It is beyond the scope of this paper to discuss this in detail here but a few remarks are in order. In the search for mirror leptons, one would like to look for characteristic signatures which can be distinguished from SM background. One of such signatures could be events with displaced vertices, in particular events with decay lengths which are macroscopic ($l > 1\,\text{mm}$). Note that displaced vertex detected outside the micro-detector with decay length $l > 1\mu$m is often regarded as a threshold for interesting phenomenology, a smoking gun signal for new physics. How this type of events can be correlated to $\mu \to e\gamma$ is a topic which was already mentioned in [3]. With the present update which includes a more detailed analysis taking into account mixings in the

JHEP12(2015)169

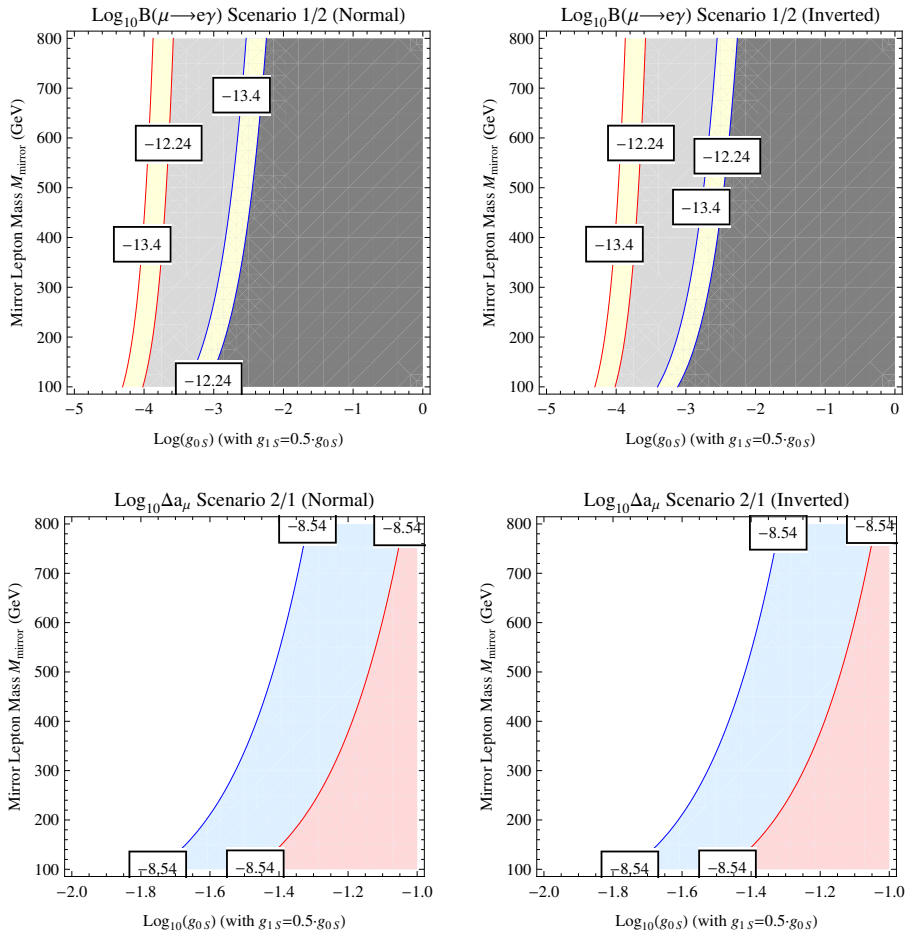

Figure 7. Same as figure 4 with $g_{0S} = g'_{0S}$ and $g_{1S} = g'_{1S} = 0.5 \cdot g_{0S}$ instead.

lepton sector, one can have a better idea of the correlation between the feasibility to observe $\mu \to e\gamma$ and the detection of mirror leptons.

A mirror lepton can decay directly into SM leptons with an accompanying Higgs singlet. For example, one can have $l^M_{Ri} \to l_{Lj} + \phi_{kS}$ where $i, j = e, \mu, \tau$ and $k = 0, 1, 2, 3$. The decay length will depend on the magnitude of the Yukawa couplings as well as on the various mixing parameters contained in eq. (4.13). We just take one example here for the sake of discussion. The interaction Lagrangian for $\mu^M_{Ri} \to l_{Lj} + \phi_{kS}$ can be expressed as $(\bar{e}_L \mathcal{M}_{12} + \bar{\mu}_L \mathcal{M}_{22} + \bar{\tau}_L \mathcal{M}_{32}) \mu^M_R$ where (for scenario 2 with the normal hierarchy)

$$\begin{aligned} \mathcal{M}_{12} = {} & (5.834 \times 10^{-6} - 0.000025i) g_{0S} \phi_{0S} + \\ & (g_{1S}(0.324 + 0.159i) + g_{2S}(0.407 - 0.171i)) \phi_{1S} + \\ & (g_{1S}(0.154 + 0.200i) + g_{2S}(0.192 + 0.238i)) \phi_{2S} + \\ & (g_{1S}(0.074 - 0.325i) + g_{2S}(0.201 - 0.102i)) \phi_{3S} \end{aligned} \tag{7.1}$$

JHEP12(2015)169

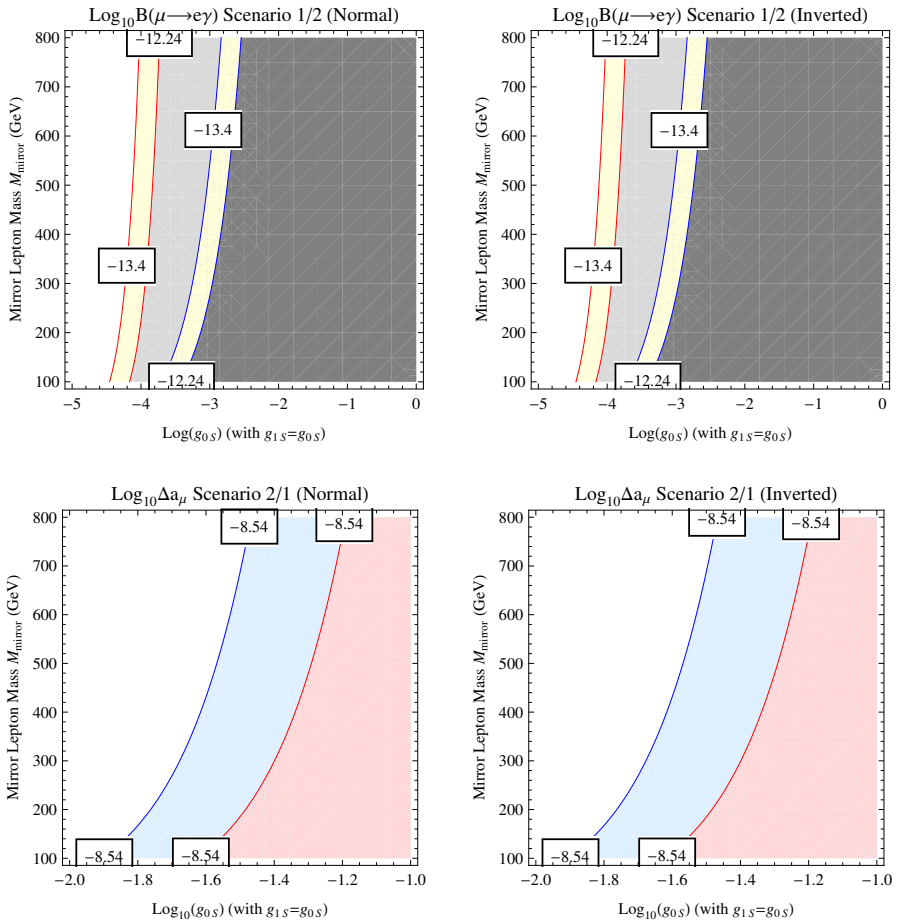

Figure 8. Same as figure 4 with $g_{0S} = g'_{0S} = g_{1S} = g'_{1S}$ instead.

$$
\begin{aligned}
\mathcal{M}_{22} = {} & 0.999933 g_{0S}\phi_{0S} + \\
& (g_{1S}(-0.262 + 0.332i) + g_{2S}(-0.262 - 0.332i))\phi_{1S} + \\
& (g_{1S}(0.146 - 0.193i) + g_{2S}(0.146 + 0.193i))\phi_{2S} + \\
& (g_{1S}(0.067 - 0.255i) + g_{2S}(0.067 + 0.255i))\phi_{3S} \\
\mathcal{M}_{32} = {} & (0.00006 + 0.00002i) g_{0s}\phi_{0S} + \\
& (g_{1S}(-0.054 - 0.276i) + g_{2S}(-0.145 + 0.257i))\phi_{1S} + \\
& (g_{1S}(-0.163 - 0.043i) + g_{2S}(0.269 + 0.405i))\phi_{2S} + \\
& (g_{1S}(0.166 - 0.503i) + g_{2S}(-0.157 - 0.077i))\phi_{3S}
\end{aligned}
$$

Depending on the particular search (e, μ or τ), a displaced vertex might occur. For instance, if one focuses on τ, and if $g_{iS} \ll g_{0S}$, the constraint on $g_{0S} < 10^{-3}$ (see the above figures) implies that $\mu^M_{Ri} \to \tau_L + \phi_{kS}$ would have a macroscopic decay length. There are many such cases but it is beyond the scope of this paper to discuss this issue at length. We merely point out the relationship between the constraints coming from $\mu \to e\gamma$ and the implication on the search for mirror leptons.

JHEP12(2015)169

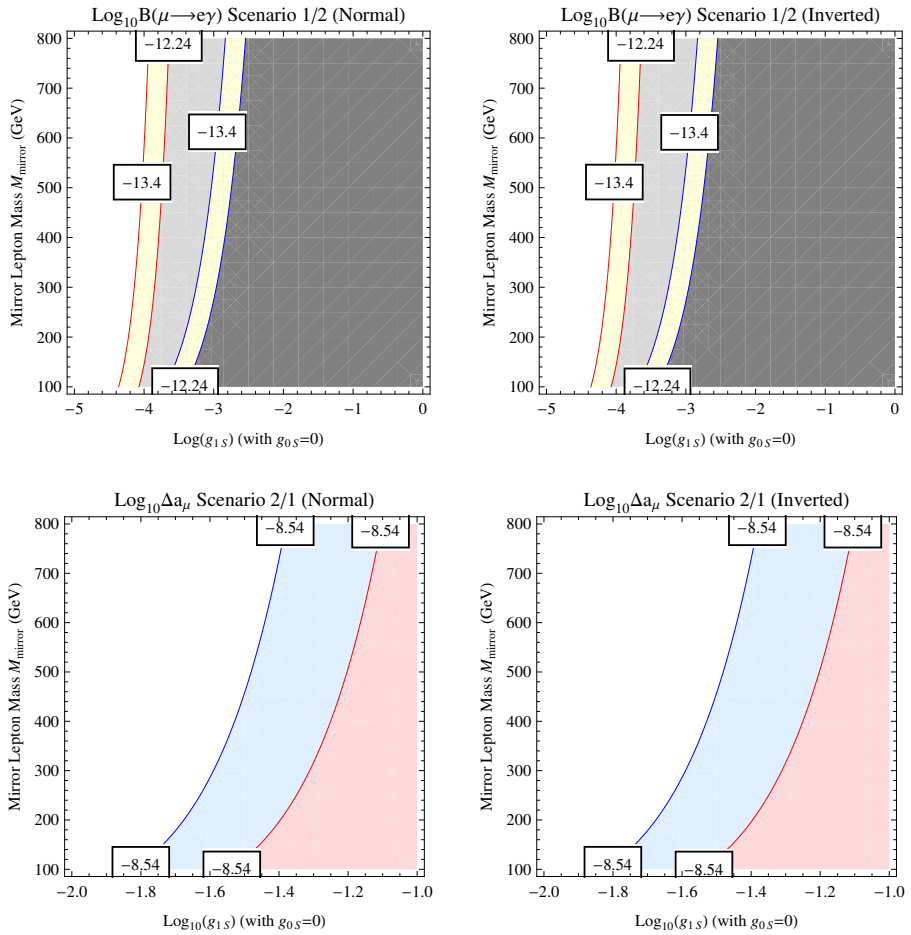

Figure 9. Same as figure 4 with $g_{0S} = g'_{0S} = 0$ and $g_{1S} = g'_{1S}$ instead.

- The other implication concerns the VEV of the singlet Higgs fields. Since the seesaw mechanism implies the masses of the light neutrinos are given by $\sim m_D^2/M$ and with $M \sim O(\Lambda_{\rm EW})$, it was stated in [1] that $m_D \sim O(100\,{\rm keV})$ and that the singlet VEV $\sim O(100\,{\rm keV})$ if $g_S \sim O(1)$. However, constraints from $\mu \to e\gamma$ imply $g_{0S} < 10^{-3}$ which now brings the singlet VEV up to $O(100\,{\rm MeV})$. In fact it can even be of the order $O(1\,{\rm GeV})$. From this observation, it is safe to say that there does not appear to be much of a hierarchy problem in the EW-scale ν_R model.

8 Conclusions

In this work, we present an update on a previous analysis [3] for the process $\mu \to e\gamma$ performed in the original EW-scale ν_R model [1] to an extended model [6]. Mixings effects of neutrinos and charged leptons constructed with a A_4 symmetry as recently studied in [7] are also taken into account. In this context, the rare process $\mu \to e\gamma$ is link to interesting new physics beyond the SM in the lepton sector, like neutrino and charged lepton mass

JHEP12(2015)169

mixings, neutrino mass hierarchies, mirror leptons as well as singlet and triplet scalars of A_4, etc. The related muon anomalous magnetic dipole moment is also studied in detail for the model.

To summarize, we find that

- One can deduce more stringent constraints on the parameter space of the EW-scale ν_R model by using the LFV process $\mu \to e\gamma$ than the muon anomalous magnetic dipole moment.

- The branching ratio $B(\mu \to e\gamma)$ shows some sensitivity to the neutrino mass hierarchies in scenario 2 but not scenario 1, depending on the A_4 triplet coupling constants. However we are not advocating the use of the process $\mu \to e\gamma$ to settle the issue of neutrino mass hierarchies.

- More stringent constraints can be deduced in scenario 1 than scenario 2 using $B(\mu \to e\gamma)$.

- Future data from MEG experiment with the projected sensitivity will impose further constraints on the parameter space of the model.

- The muon anomalous magnetic dipole moment is sensitive neither to the neutrino mass hierarchies nor the scenarios for all 6 cases of the couplings studied here for the model.

Searching for new physics via rare processes is complementary to direct production of new particles at colliders. For $\mu \to e\gamma$, the relevant new particles in the model are the mirror leptons and scalar singlets running inside the loop diagram. As shown in our analysis, the Yukawa couplings of the Higgs singlets to the leptons in the EW-scale ν_R model are constrained to be small in order to be consistent with the current experimental limit on $B(\mu \to e\gamma)$. Thus searching for mirror particles of this model at the LHC would be quite interesting since, due to small couplings, they might decay outside the beam pipe and inside the silicon vertex detectors. The A_4 singlet and triplet scalars are likely to escape detection as missing energies.

As an outlook, one would like to generalize this work to $\mu - e$ conversion. This work is now in progress and will be reported elsewhere [34].

A Useful formulas

For the general case of retaining the external fermion masses $m_{i,j}$, the factors of $m_i \mathcal{I}\left(\frac{m^2_{\phi_{kS}}}{m^2_{l^M_m}}\right)$, $m_j \mathcal{I}\left(\frac{m^2_{\phi_{kS}}}{m^2_{l^M_m}}\right)$ and $\mathcal{J}\left(\frac{m^2_{\phi_{kS}}}{m^2_{l^M_m}}\right)$ in eqs. (5.7)–(5.8) for $C^{ij}_{L,R}$ should be replaced by $m_i \mathcal{I}_1\left(\frac{m^2_{\phi_{kS}}}{m^2_{l^M_m}}, \frac{m^2_i}{m^2_{l^M_m}}, \frac{m^2_j}{m^2_{l^M_m}}\right)$, $m_j \mathcal{I}_2\left(\frac{m^2_{\phi_{kS}}}{m^2_{l^M_m}}, \frac{m^2_i}{m^2_{l^M_m}}, \frac{m^2_j}{m^2_{l^M_m}}\right)$ and $\mathcal{J}\left(\frac{m^2_{\phi_{kS}}}{m^2_{l^M_m}}, \frac{m^2_i}{m^2_{l^M_m}}, \frac{m^2_j}{m^2_{l^M_m}}\right)$ respec-

JHEP12(2015)169

tively, where

$$\mathcal{I}_1(r,r_i,r_j) = \int_0^1 dx \int_0^{1-x} dy \frac{y(1-x-y)}{x+y+(1-x-y)(r-xr_j-yr_i)-i0^+} ,$$
$$\mathcal{I}_2(r,r_i,r_j) = \int_0^1 dx \int_0^{1-x} dy \frac{x(1-x-y)}{x+y+(1-x-y)(r-xr_j-yr_i)-i0^+} ,$$
$$\mathcal{J}(r,r_i,r_j) = \int_0^1 dx \int_0^{1-x} dy \frac{x+y}{x+y+(1-x-y)(r-xr_j-yr_i)-i0^+} .$$

Acknowledgments

We would like to thank the hospitality of The International Center of Interdisciplinary Science Education (ICISE) at Quy Nhon, Vietnam, where this project was completed. TL would like to thank the hospitality of the Institute of Physics, Academia Sinica, Taiwan where part of this project was carried out. This work was supported in part by the Ministry of Science and Technology (MoST) of Taiwan under grant numbers 101-2112-M-001-005-MY3 and 104-2112-M-001-001-MY3, by US DOE grant DE-FG02-97ER41027 and by the Pirrung Foundation.

References

[1] P.Q. Hung, *A Model of electroweak-scale right-handed neutrino mass*, *Phys. Lett.* **B 649** (2007) 275 [hep-ph/0612004] [INSPIRE].

[2] V. Hoang, P.Q. Hung and A.S. Kamat, *Electroweak precision constraints on the electroweak-scale right-handed neutrino model*, *Nucl. Phys.* **B 877** (2013) 190 [arXiv:1303.0428] [INSPIRE].

[3] P.Q. Hung, *Electroweak-scale mirror fermions, $\mu \to e\gamma$ and $\tau \to \mu\gamma$*, *Phys. Lett.* **B 659** (2008) 585 [arXiv:0711.0733] [INSPIRE].

[4] ATLAS collaboration, *Observation of a new particle in the search for the Standard Model Higgs boson with the ATLAS detector at the LHC*, *Phys. Lett.* **B 716** (2012) 1 [arXiv:1207.7214] [INSPIRE].

[5] CMS collaboration, *Observation of a new boson at a mass of 125 GeV with the CMS experiment at the LHC*, *Phys. Lett.* **B 716** (2012) 30 [arXiv:1207.7235] [INSPIRE].

[6] V. Hoang, P.Q. Hung and A.S. Kamat, *Non-sterile electroweak-scale right-handed neutrinos and the dual nature of the 125-GeV scalar*, *Nucl. Phys.* **B 896** (2015) 611 [arXiv:1412.0343] [INSPIRE].

[7] P.Q. Hung and T. Le, *On neutrino and charged lepton masses and mixings: A view from the electroweak-scale right-handed neutrino model*, *JHEP* **09** (2015) 001 [*Erratum ibid.* **1509** (2015) 134] [arXiv:1501.02538] [INSPIRE].

JHEP12(2015)169

[8] E. Ma, *A_4 Symmetry and Neutrinos*, *Int. J. Mod. Phys.* **A 23** (2008) 3366 [arXiv:0710.3851] [INSPIRE].

[9] E. Ma and G. Rajasekaran, *Softly broken A_4 symmetry for nearly degenerate neutrino masses*, *Phys. Rev.* **D 64** (2001) 113012 [hep-ph/0106291] [INSPIRE].

[10] S.F. King and C. Luhn, *Neutrino Mass and Mixing with Discrete Symmetry*, *Rept. Prog. Phys.* **76** (2013) 056201 [arXiv:1301.1340] [INSPIRE].

[11] J.C. Pati and A. Salam, *Lepton Number as the Fourth Color*, *Phys. Rev.* **D 10** (1974) 275 [*Erratum ibid.* **D 11** (1975) 703] [INSPIRE].

[12] R.N. Mohapatra and J.C. Pati, *A Natural Left-Right Symmetry*, *Phys. Rev.* **D 11** (1975) 2558 [INSPIRE].

[13] G. Senjanović and R.N. Mohapatra, *Exact Left-Right Symmetry and Spontaneous Violation of Parity*, *Phys. Rev.* **D 12** (1975) 1502 [INSPIRE].

[14] G. Senjanović, *Spontaneous Breakdown of Parity in a Class of Gauge Theories*, *Nucl. Phys.* **B 153** (1979) 334 [INSPIRE].

[15] CMS collaboration, *Measurement of Higgs boson production and properties in the WW decay channel with leptonic final states*, *JHEP* **01** (2014) 096 [arXiv:1312.1129] [INSPIRE].

[16] CMS collaboration, *Measurement of the properties of a Higgs boson in the four-lepton final state*, *Phys. Rev.* **D 89** (2014) 092007 [arXiv:1312.5353] [INSPIRE].

[17] CMS collaboration, *Search for the standard model Higgs boson produced in association with a W or a Z boson and decaying to bottom quarks*, *Phys. Rev.* **D 89** (2014) 012003 [arXiv:1310.3687] [INSPIRE].

[18] CMS collaboration, *Evidence for the 125 GeV Higgs boson decaying to a pair of τ leptons*, *JHEP* **05** (2014) 104 [arXiv:1401.5041] [INSPIRE].

[19] A. Aranda, J. Hernandez-Sanchez and P.Q. Hung, *Implications of the discovery of a Higgs triplet on electroweak right-handed neutrinos*, *JHEP* **11** (2008) 092 [arXiv:0809.2791] [INSPIRE].

[20] S. Chakdar, K. Ghosh, V. Hoang, P.Q. Hung and S. Nandi, *The search for mirror quarks at the LHC*, arXiv:1508.07318 [INSPIRE].

[21] N. Cabibbo, *Time Reversal Violation in Neutrino Oscillation*, *Phys. Lett.* **B 72** (1978) 333 [INSPIRE].

[22] L. Wolfenstein, *Oscillations Among Three Neutrino Types and CP-violation*, *Phys. Rev.* **D 18** (1978) 958 [INSPIRE].

[23] S.T. Petcov, *The Processes $\mu \to e\gamma$, $\mu \to ee\bar{e}$, Neutrino' $\to$ Neutrino γ in the Weinberg-Salam Model with Neutrino Mixing*, *Sov. J. Nucl. Phys.* **25** (1977) 340 [*Erratum ibid.* **25** (1977) 698] [INSPIRE].

[24] T.P. Cheng and L.-F. Li, *Nonconservation of separate mu-lepton and e-lepton numbers in gauge theories with v+a currents*, *Phys. Rev. Lett.* **38** (1977) 381 [INSPIRE].

[25] B.W. Lee and R.E. Shrock, *Natural Suppression of Symmetry Violation in Gauge Theories: Muon-Lepton and Electron Lepton Number Nonconservation*, *Phys. Rev.* **D 16** (1977) 1444 [INSPIRE].

[26] W.J. Marciano and A.I. Sanda, *Exotic Decays of the Muon and Heavy Leptons in Gauge Theories*, *Phys. Lett.* **B 67** (1977) 303 [INSPIRE].

JHEP12(2015)169

[27] J.-P. Bu, Y. Liao and J.-Y. Liu, *Lepton Flavor Violating Muon Decays in a Model of Electroweak-Scale Right-Handed Neutrinos*, *Phys. Lett.* **B 665** (2008) 39 [arXiv:0802.3241] [INSPIRE].

[28] PARTICLE DATA GROUP collaboration, K.A. Olive et al., *Review of Particle Physics*, *Chin. Phys.* **C 38** (2014) 090001 [INSPIRE].

[29] F. Capozzi, G.L. Fogli, E. Lisi, A. Marrone, D. Montanino and A. Palazzo, *Status of 3ν oscillation parameters at the end of 2013*, *J. Phys. Conf. Ser.* **598** (2015) 012002 [INSPIRE].

[30] F. Capozzi, G.L. Fogli, E. Lisi, A. Marrone, D. Montanino and A. Palazzo, *Status of three-neutrino oscillation parameters, circa 2013*, *Phys. Rev.* **D 89** (2014) 093018 [arXiv:1312.2878] [INSPIRE].

[31] MEG collaboration, J. Adam et al., *New constraint on the existence of the $\mu^+ \to e^+\gamma$ decay*, *Phys. Rev. Lett.* **110** (2013) 201801 [arXiv:1303.0754] [INSPIRE].

[32] MEG collaboration, F. Renga, *Latest results of MEG and status of MEG-II*, arXiv:1410.4705 [INSPIRE].

[33] A. Hoecker and W.J. Marciano, http://pdg.lbl.gov/2013/reviews/rpp2013-rev-g-2-muon-anom-mag-moment.pdf.

[34] P.Q. Hung, T. Le, V.Q. Tran and T.C. Yuan, *Mu-to-e conversion in EW-scale ν_R model*, work in progress.

JHEP12(2015)169